

Chapter 3

Microstructural Design of Lead Oxide–Epoxy Composites for Radiation Shielding Purposes



Abstract Composite epoxy samples filled with PbO and Pb₃O₄ were fabricated to investigate the mass attenuation characteristics of the composites to X-rays in the diagnostic imaging energy range. The effect of density on the attenuation ability of the composites for radiation shielding purposes was studied using a calibrated X-ray machine. Characterization of the microstructure properties of the synthesized composites was performed using synchrotron radiation diffraction, optical microscopy, and scanning electron microscopy. The results indicate that the attenuation ability of the composites increased with an increase in density. The particle size of WO₃ fillers has a negligible effect on the value of mass attenuation coefficient. Microstructural analyses have confirmed the existence of uniform dispersion of fillers within the matrix of epoxy matrix with the average particle size of 1–5 μm for composites with filler loading of ≤30 wt% and 5–15 μm for composites with filler loading of ≥50 wt%.

3.1 Introduction

During the early part of the 20th century, the hazards from ionizing radiation were recognized, and the use of lead and other materials became commonplace for shielding against X-rays [1–3]. Once the dangers of X-rays are considered, lead has become an important material for radiation protection. Since then protection has evolved into an elaborate infrastructure of controls and disciplines specifying how this shield should be deployed [4–6]. Recently, shielding requirements have become more stringent as standards for exposure of personnel and the general public. X-ray technologists practice a principle called as-low-as-reasonably-achievable dose when dealing with X-rays, so that radiation dose received by personnel and the general public can be as low as possible [3–7].

The shielding for radiation purposes are based on the type and energy of the radiation itself. Gamma and X-rays are the most penetrating radiations as compared to other ionizing radiations. Their interaction depends on the probability of their collision with the atoms of the materials during the interaction. To increase the probability, they will interact the density of the material they are passing through

needs to be increased which means the materials should have a lot of atoms with an assumption that the materials are free from voids. If dealing with a material having a lot of pores, porosity needs to be considered, because it will affect the interaction of the radiations with the atoms within the material [8].

Lead-glass is one example of the material used as shielding materials for ionizing radiations, but it is heavy, expensive, and very brittle. So, it is not surprising that polymers have made inroads into markets that were in the beginning dominated by glass. Polymers also have a great potential in many important applications that glass could not meet because of their unique properties, such as a low density, ability to form intricate shapes, optical transparency, low manufacturing cost, and toughness. However, the use of polymers is still limited, because of their inherent softness and low thermal stability [9, 10]. One modern example of the filler-reinforced polymer used for radiation shielding is lead-acrylic [11, 12]. Moreover, many researchers tried to create new lead-based composites for this radiation shielding purposes such as lead-polyester composites [13], lead-styrene butadiene rubber [14], lead-polystyrene [15], and similar materials.

Rudraswamy et al. [16] have shown that some lead compounds such as PbO , PbO_2 , PbNO_3 , and PbCl_2 have an adequate mass attenuation coefficient, lm for use in radiation shielding purposes. Unfortunately, the usage of either lead or lead compounds alone will cause certain health risks to human, animals, and to the surroundings [17]. Moreover, lead or lead compounds themselves are also not malleable and lack in mechanical strength [18].

Additionally, there are many methods available to achieve a good dispersion of fillers within a polymeric matrix. One of the traditional methods for dispersing fillers in polymer matrices is melt-mixing method of the fillers into the polymer. The fillers are weighted and added straightly into the polymer for mixing. In many works done, many researchers used a static mixer with constant speed during the mixing process to achieve homogenously dispersion of fillers within the polymers [13, 19]. It is expected that lead oxide–epoxy composites will be a good material to be used as radiation shielding in diagnostic radiology purposes. This is because lead oxide can be easily dispersed within a polymer matrix [13]. Besides, an epoxy system is a thermoset material that is generally stronger and better suited to higher temperatures than thermoplastics, so it can withstand the high energetic X-rays bombardment during the diagnostic imaging [20]. Hence, the purpose of this study is to prepare and characterize a composite that is made of an epoxy system filled with lead oxides. The feasibility of this material for use in X-ray shielding is discussed.

3.2 Results and Discussion

3.2.1 Density of Samples

As can be seen from Table 3.1, the values of apparent density for samples obtained

Table 3.1 Comparison of measured and theoretical density values for the composites

Composite designation	Density of composite, ρ_{comp} (g/cm ³)	
	Theoretical	Measured
A1	1.26	1.26 ± 0.01
A2	1.56	1.53 ± 0.01
A3	2.06	2.05 ± 0.02
A4	3.00	2.93 ± 0.03
B1	1.26	1.26 ± 0.01
B2	1.55	1.55 ± 0.01
B3	2.02	2.00 ± 0.03
B4	2.90	2.83 ± 0.03

from the Archimedes’ technique did not totally agreed with the theoretical values because of experimental uncertainties. The porosity calculated for each sample was less than 1%. Besides, the higher the wt% of the filler within the composite, the higher the value of q_c as also been observed by Harish et al. [13], Berger et al. [21].

3.2.2 X-Ray Mass Attenuation Coefficients

The μ_m values given in NIST are specifically measured for characteristic photon energy, whereas in this experiment; the X-ray tube voltages used are in continuous spectrum. So, the equivalent energies for the X-ray tube voltages used within the experiment must be taken into account for comparing the value of l_m between NIST and experiment. The equivalent energies for the X-rays tube voltages used are shown in Table 3.2. These values were calculated using the equation fitted as an exponential function (Eq. 3.1) [22]:

$$y = a_{\text{exp}}^{-\left(\frac{x}{c}\right)} + b \tag{3.1}$$

Table 3.2 Equivalent energy for the various X-ray tube voltages used

X-ray tube voltage (kV _p)	Equivalent energy (keV)
40	29.9
50	34.3
60	38.5
70	42.5
80	46.2
90	49.7
100	52.9

where a , b , and c in the Eq. (3.2) are constants with values of -97.535 , 106.857 , and 168.672 , respectively, whereas y is the equivalent energy and x is the X-ray tube voltage. For composites, the value of μ_m was calculated using Eq. (3.2):

$$\mu_m = \sum w_i \mu_{m_i} \quad (3.2)$$

where μ_m is the mass attenuation coefficient of the composite, whereas w_i and μ_{m_i} are the weight fraction and the mass attenuation coefficient of each compound used to make the composite, respectively.

The plots in Fig. 3.1a–c show that almost all the lines for the l_m experimental values were a few percent lower than the l_m values interpolated from NIST for the given X-ray tube voltages. These results are like the work done by Gerward et al., which they have found that tabulated X-ray mass attenuation coefficients are commonly a few percent higher than the measured values [23, 24]. Icelli et al. [25] obtained very similar results where the higher the density of the material, the higher the value of μ_m . However, the relationship between mass attenuation coefficient (l_m) and particle size of lead oxide remains unknown. The use of nanosized lead oxide increase or decrease the value of μ_m ? As nanosized lead oxide was not available, the effect of particle size of WO_3 filler (purchased from Sigma–Aldrich, Castle Hill, NSW, Australia) on μ_m was studied. The procedure to prepare this composite was similar to that for preparing PbO –epoxy samples. Figure 3.1d shows the effect of particle size on the mass attenuation coefficient in epoxy composite filled with either microsized ($\sim 20 \mu m$) or nanosized ($< 100 \text{ nm}$) WO_3 . It is clearly shown that particle size has a negligible effect on the value of μ_m of a material for this range of X-ray energy 40–100 kVp. However, it should be noted that nanosized particles (e.g., CuO) have been reported to show better X-ray attenuation at the lower X-ray beam energy (i.e., 26–30 kV) [26, 27]. As photoelectric absorption dominates at low photon energies, the probability of an X-ray with low energy to interact and to be absorbed is higher for nanosized particles, in addition to maximization of the surface/volume ratio. However, as photon energy increases, the probability of Compton scattering increases, and hence the attenuation by the material decreases, as this interaction is weakly dependent on atomic number of the element and the photon energy. Hence, the probability of an X-ray with higher energy to interact and to be absorbed becomes similar for both nanosized and microsized particles. It appears that the use of nanosized particles only helps in providing a uniform dispersion within the epoxy matrix but has no direct effect on the value of μ_m as clearly indicated in Eq. (3.2). Only the abundance of WO_3 dispersed in the composite will influence the value of μ_m . The mass attenuation coefficient, μ_m is the rate of photon interactions within 1-unit of mass per 1-unit of area (g/cm^2). It depends on the energy of the photon and the concentration of electrons in the material. Its value will decrease rapidly with the increment of photon energy. Further the chance of a photon coming close enough to an electron is higher when the concentration of electrons within the material is higher, because it is absorbed by the material. Electron concentration was determined by the physical density of the material. Thus, composites with a fine

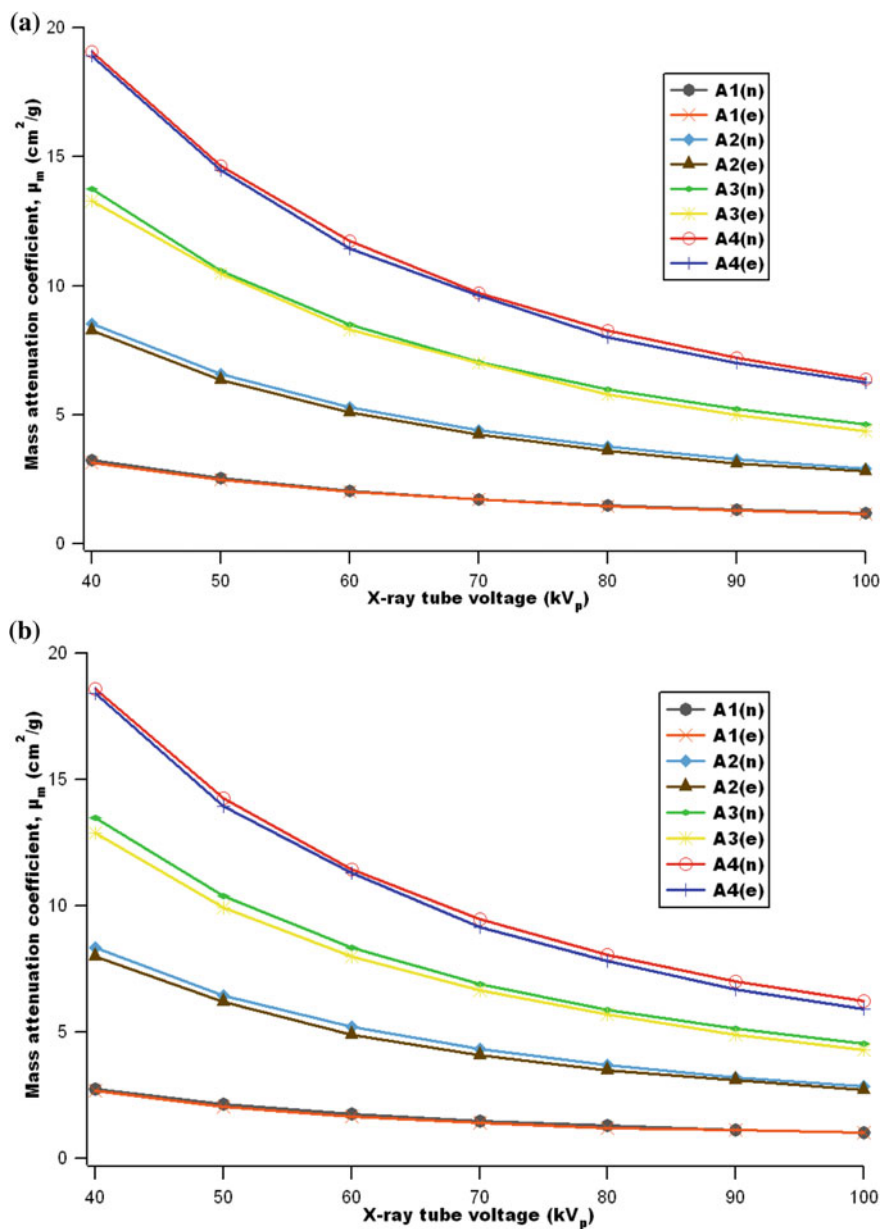


Fig. 3.1 Mass attenuation coefficients as a function of kV_p as obtained from NIST (n) and experiment (e) for samples of **a** PbO-epoxy composite, **b** Pb_3O_4 -epoxy composite, **c** close-up view of (a), and **d** micro- and nano- WO_3 epoxy composites [29]

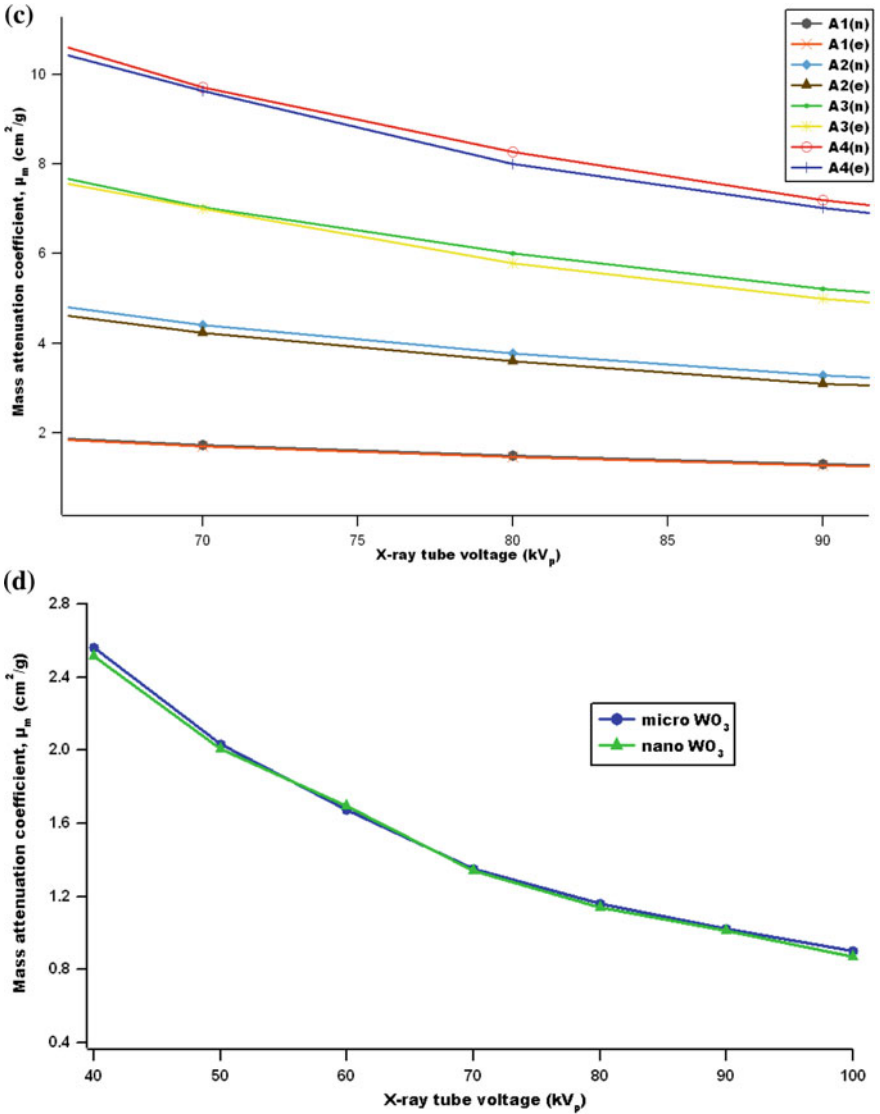


Fig. 3.1 (continued)

dispersion of high-density material provide more interaction probability for photons and also better radiations shielding properties [13, 28]. To ascertain the shielding ability of the composites, calculations of μ_m were done to compare the 50 wt% of PbO reinforced isophthalate resin composite performed by Harish et al. [13] The value of μ_m for their composite was calculated to be $0.0948 \text{ cm}^2/\text{g}$, whereas the values of μ_m for samples A3 and B3 in this study, which also have 50 wt% of the

Table 3.3 Mass attenuation coefficients interpolated from NIST databases for gamma rays of energy 0.662 MeV from Cs-137 point source

Composite designation	Mass attenuation coefficient, μ_m (cm ² /g)
A1	0.0871
A2	0.0924
A3	0.0978
A4	0.1055

fillers, were 0.0978 and 0.0974 cm²/g, respectively. The calculation of μ_m was done by interpolating NIST databases for gamma rays of energy 0.662 MeV from a Cs-137-point source. These results show that samples A3 and B3 in this study provided better radiation shielding than the composite fabricated by Harish and coworkers. Moreover, the usage of lead oxides for radiation shielding can be minimal in the fabrication of composites and thus reduce the health risks associated with lead oxides. The results for other samples at the same energy range are shown in Table 3.3.

3.2.3 Phase Compositions

The reference for phase-fitting the peaks were taken from International Centre for Diffraction Data PDF-4 + 2009 database. The wavelength for all these databases was chosen to be the same as the wavelength of the synchrotron radiation used. From Fig. 3.2a, all the peaks belong to orthorhombic PbO crystal structures (PDF_4 p files 01-076-1796). While for composite filled with Pb₃O₄ powder, all the peaks were identified as tetragonal Pb₃O₄ crystal structures (PDF-4 + file 04-007-2162) as shown in Fig. 3.2b. These indicate that the powders of PbO and Pb₃O₄ used were single-phase pure.

3.2.4 Microstructures

The typical fracture surfaces for the samples are shown in Fig. 3.3. The scratches seen in the images were due to the polishing process. These images have shown that the fractured surfaces were quite rough, and the fillers (white patches) were well dispersed and firmly embedded in the epoxy matrix due to their relatively small particle size and good compatibility with the epoxy matrix. Although the fillers have a greater weight fraction than epoxy, they were dispersed quite uniformly with only some agglomerations to be found. As can be seen in Fig. 3.3a, the blurry white patches are clear indications of some minor filler agglomerations. The scanning electron microscopy (SEM) images in Fig. 3.4 have provided results that agreed with the optical images shown in Fig. 3.3. The bright regions represent the filler particles (lead-oxide) dispersed in the dark epoxy matrix. The fillers were seen to be

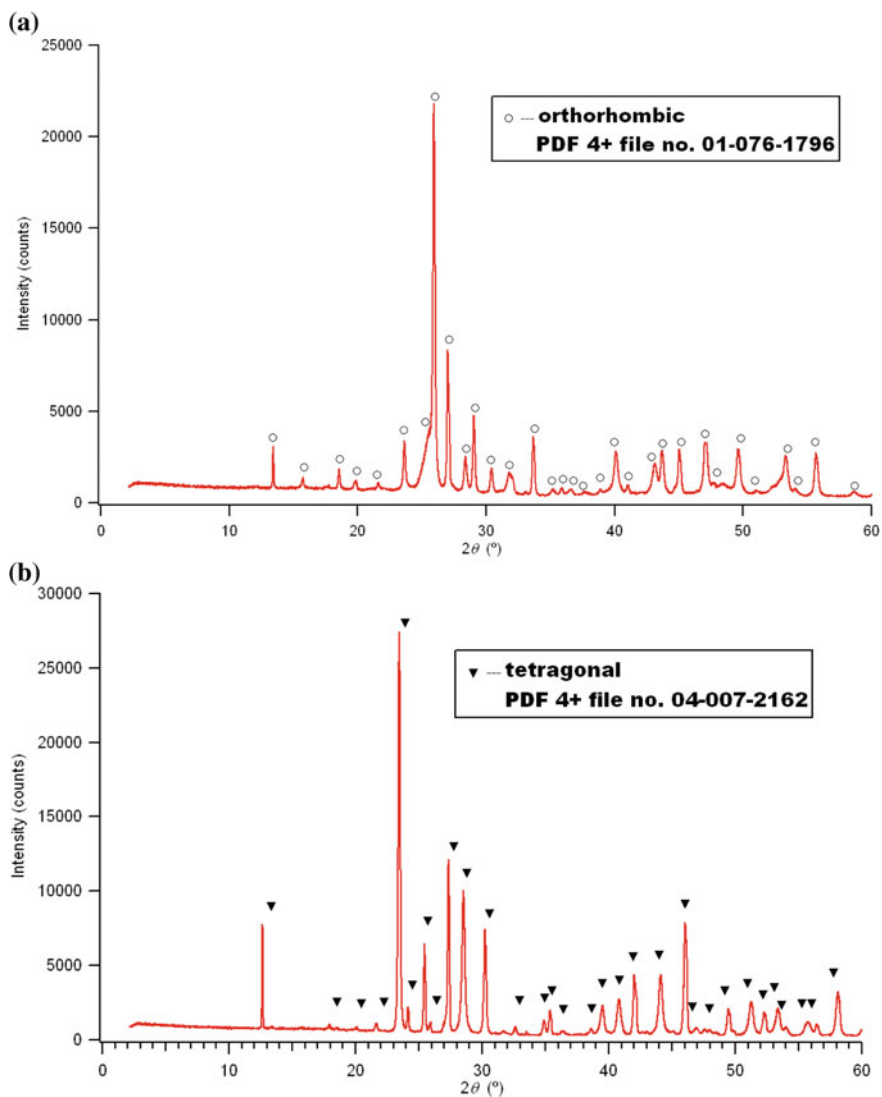


Fig. 3.2 Typical powder diffraction patterns for **a** PbO–epoxy composite and **b** Pb₃O₄–epoxy composite [29]

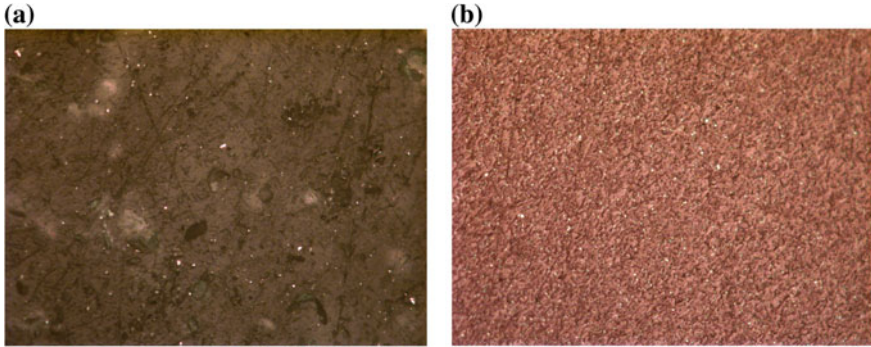


Fig. 3.3 Optical micrographs showing the typical uniform dispersion of fillers in the matrix of epoxy for two composite samples: **a** A3 and **b** B2. 50 × magnification [29]

quite uniformly dispersed in the composites, although minor agglomerations can be observed. The average particle size obtained from the SEM images was $\sim 1\text{--}5\ \mu\text{m}$ for composites with filler loading of $\leq 30\ \text{wt}\%$ and $\sim 5\text{--}15\ \mu\text{m}$ for composites with filler loading of $\geq 50\ \text{wt}\%$.

3.3 Conclusions

Epoxy composites filled with dispersed lead oxide particles of $1\text{--}5\ \mu\text{m}$ for composites with filler loading of $\leq 30\ \text{wt}\%$ and $5\text{--}15\ \mu\text{m}$ for composites with filler loading of $\geq 50\ \text{wt}\%$ have been successfully fabricated. These composites showed good X-ray attenuation properties and could be considered as a potential candidate for radiation shielding in diagnostic radiology purposes. The particle size of WO_3 fillers has a negligible effect on the value mass attenuation coefficient (μ_m) for the X-ray energy of $40\text{--}100\ \text{kVp}$. In addition, the lead oxide–epoxy composites in this study are superior to the lead oxide–isophthalate resin composite previously investigated.

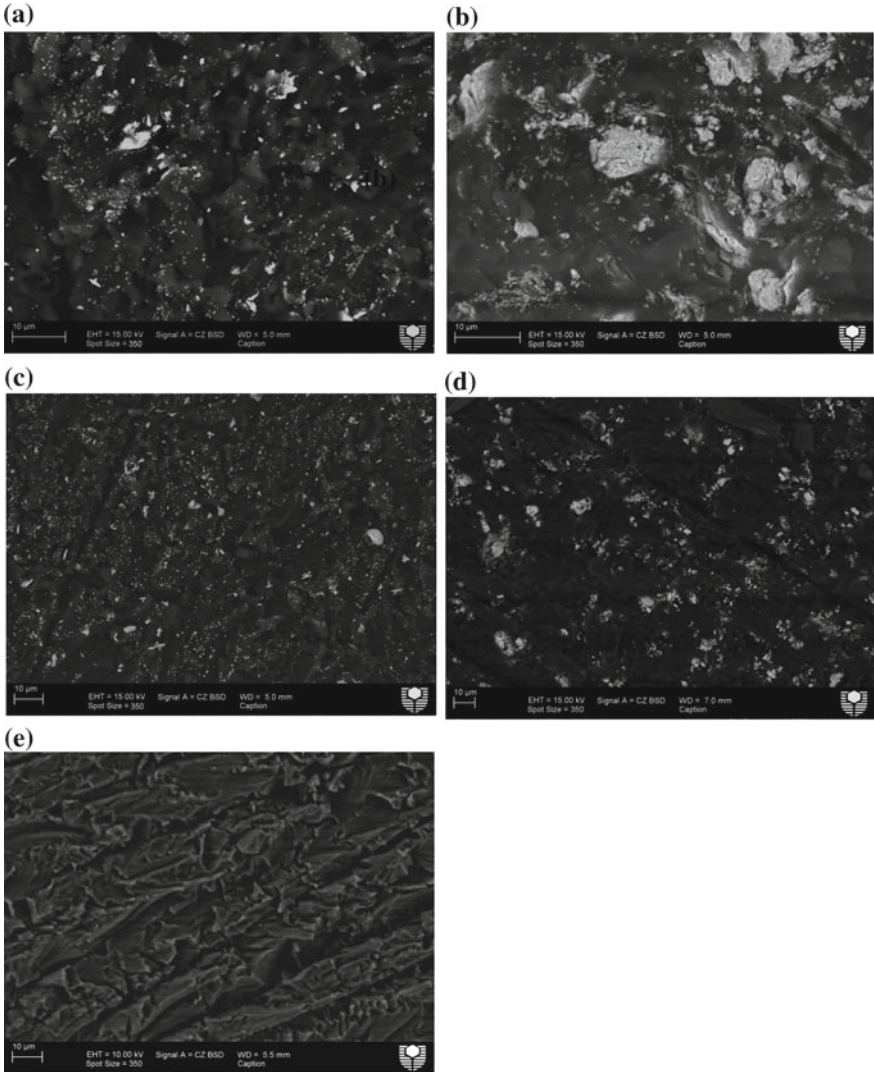


Fig. 3.4 SEM micrographs showing the uniform dispersion of PbO or Pb₃O₄ particles within the epoxy matrix in various composite samples: **a** A3, **b** A4, **c** B2, **d** B3, and **e** pure epoxy [29]

Acknowledgements The funding for the collection of synchrotron powder diffraction data at the Australian Synchrotron in this work was provided by Grant Number AS111/PD3509 and AS111_PDFI3181.

References

1. Archer BR, Thornby JI, Bushong SC (1983) Diagnostic X-ray shielding design based on an empirical model of photon attenuation. *Health Phys* 44:507
2. Archer BR (1995) History of the shielding of diagnostic X-ray facilities. *Health Phys* 69:750
3. Archer BR (2005) Recent history of the shielding of medical X-ray imaging facilities. *Health Phys* 88:579
4. Hessenbruch A (2002) A brief history of x-rays. *Endeavour* 26:137
5. Okunade AA (2002) Comparison of lead attenuation and lead hardening equivalence of materials used in respect of diagnostic X-ray shielding. *Appl Radiat Isot* 57:819
6. Okunade AA (2004) Numerical models for the determination of primary structural barriers for diagnostic X-ray facilities. *Med Phys* 31:513
7. Dixon RL, Simpkin DJ (1998) Primary shielding barriers for diagnostic X-ray facilities: a new model. *Health Phys* 74:181
8. Lorenzen W (2000) Is Gold better than lead as a radiation shield. *MadSci network: engineering*
9. Polymer versus Glass, POLYMICRO Newsletter, 2004. Available at: <http://www.polymicro-cc.com>. Accessed on 24 June 2011
10. Lee EH, Rao GR, Lewis MB, Mansur LK (1993) Ion beam application for improved polymer surface properties. *Nucl Instrum Methods Phys Res Sect B: Beam Interact Mater Atoms* 74:326
11. Premac Lead Acrylic, Part of the Wardray Premise Total Radiation Shielding Package, Wardray Premise Ltd. Available at: <http://wardray-premise.com/structural/materials/premac.html>. Accessed on 4 May 2011
12. Radiation Safety & Consumable Products. Available at: http://www.lablogic.com/moreinfo/PDF/consumables/lablogic_consumables_brochure.pdf. Accessed on 4 May 2011
13. Harish V, Nagaiah N, Prabhu TN, Varughese KT (2009) Preparation and characterization of lead monoxide filled unsaturated polyester based polymer composites for gamma radiation shielding applications. *J Appl Polym Sci* 112:1503
14. Abdel-Aziz MM, Badran AS, Abdel-Hakem AA, Helaly FM, Moustafa AB (1991) Styrene-butadiene rubber/lead oxide composites as gamma radiation shields. *J Appl Polym Sci* 42:1073
15. Pavlenko VI, Lipkanskii VM, Yastrebinskii PN (2004) Calculations of the passage of gamma-quanta through a polymer radiation-protective composite. *J Eng Phys Thermophys* 77:11
16. Rudraswamy B, Dhananjaya N, Manjunatha H (2010) Measurement of absorbed dose rate of gamma radiation for lead compounds. *Nucl Instrum Methods Phys Res Sect A: Accelerators Spectrometers Detectors Assoc Equip* 619:171
17. Robert RD (2005) High density composites replace lead. *Ecomass Technologies, Austin*
18. Spinks JWT, Wood RJ (1976) *An introduction to radiation chemistry*. Wiley-Interscience, New York
19. Tanahashi M (2010) Development of fabrication methods of filler/polymer nanocomposites: with focus on simple melt-compounding-based approach without surface modification of nanofillers. *Materials* 3:1593
20. Material Guide, Archos LLC. Available at: http://www.archosllc.com/Material_Guide_2.html. Accessed on 20 June 2011
21. Berger MJ, Hubbell JH, Seltzer SM, Chang J, Coursey JS, Sukumar R, Zucker DS, Olsen K (2010) XCOM: photon cross section database (version 1.5). National Institute of Standards and Technology, Gaithersburg, MD, 2010. Available at: <http://physics.nist.gov/xcom>. Accessed on 20 June 2011
22. Mincong C, Hongmei L, Ziyu C, Ji S (2008) An examination of mass thickness measurements with X-ray sources. *Appl Radiat Isot* 66:1387
23. Gerward L (1992) Theoretical upper and lower limits to experimental X-ray attenuation coefficients. *Nucl Inst Methods Phys Res B* 69:407
24. Midgley SM (2005) Measurements of X-ray linear attenuation coefficient for low atomic number, materials at energies 32–66 and 140 keV. *Radiat Phys Chem* 72:525
25. Icelli O, Erzeneoglu S, Boncukc-uoglu R (2004) Experimental studies on measurements of mass attenuation coefficients of boric acid at different concentration. *Ann Nucl Energy* 31:97

26. Botelho MZ, Kuñzel R, Okuno E, Levenhagen RS, Basegio T, Bergmann CP (2011) X-ray transmission through nanostructured and microstructured CuO materials. *Appl Radiat Isot* 69:527
27. Kuñzel R, Okuno E (2012) Effects of the particle sizes and concentrations on the X-ray absorption by CuO compounds. *Appl Radiat Isot* 70:781
28. Sprawls P (1993) *The physical principles of medical imaging*. Aspen Publishers, Gaithersburg
29. Noor Azman NZ, Siddiqui SA, Hart R, Low I (2012) Microstructural design of lead oxide-epoxy composites for radiation shielding performances. *M J Appl Polym Sci* 128:3213